Hindawi
Advances in Civil Engineering
Volume 2019, Article ID 1487156, 10 pages
https://doi.org/10.1155/2019/1487156

Research Article

Dynamic Compression Properties and Deterioration of Red-Sandstone Subject to Cyclic Wet-Dry Treatment

Bin Du,[1,2,3] Haibo Bai ,[1] and Guangming Wu[1]

[1]*State Key Laboratory for Geomechanics and Deep Underground Engineering, China University of Mining and Technology, Xuzhou 221116, Jiangsu, China*
[2]*Institute of Architectural Engineering Technology, Jiangsu Vocational Institute of Architectural Technology, Xuzhou, Jiangsu 221116, China*
[3]*Jiangsu Collaborative Innovation Center for Building Energy Saving and Construction Technology, Xuzhou, Jiangsu 221116, China*

Correspondence should be addressed to Haibo Bai; hbbai@126.com

Received 3 September 2018; Accepted 28 October 2018; Published 23 January 2019

Guest Editor: Dengke Wang

Rock engineering is usually associated with impact loads induced by blasting, drilling, vibration, or earthquake. In the engineering fields of tunnelling, slopes, dams, and mining, rocks are always subjected to cyclic wet-dry caused by periodical variation in moisture. To study cyclic wet-dry effects on dynamic compression properties and deterioration of red-sandstone, physical tests and dynamic and static tests were conducted after 0, 5, 10, 15, and 20 wet-dry cycles. Changes in physical and mechanical parameters, including P-wave velocity, density, and static and dynamic compression strength, were determined. Deterioration of red-sandstone caused by wet-dry cycles was verified through physicomechanical parameters, and the microscopic features were scanned by SEM techniques. Experimental results showed that the dynamic compression strength increased with the loading rate, but decreased with the increase of wet-dry cycles. In terms of the loading rate, the decay function model was proposed to evaluate the long-term dynamic compression strength of red-sandstone against cyclic wet-dry action. Besides, the function of the loading rate was obtained. Parameters of two models, decay constant and half-life values, were measured accurately.

1. Introduction

Weathering is defined as the alteration and destruction process of physical and chemical effects on rock and soil materials at or near the earth's surface. This phenomenon is widespread in rock materials [1–3]. Due to the deterioration induced by various weathering treatments, the assessment on engineering properties of rock mass is significantly important. As a typical type of the weathering process, cyclic wet and dry are prevalent in rock engineering, especially in fields of tunnelling, slopes, dams, and mining, where rock materials are usually subjected to periodical changes in the moist condition (namely, seasonal changes in groundwater level, water level changes in reservoirs, recurrent rainfall, and ebb and flow of tides) [4, 5]. Several test methods have been developed in the past decades to simulate the cyclic wet and dry actions [6–11]. Actually, an intact cycle of wet-dry consists of wet process (the transition from dry to wet) and dry process (the transition from wet to dry) [5]. To accelerate the simulation process, the wet process is usually conducted by submerging rock materials in water for different time (e.g., 12 h, 24 h, 32 h, 48 h, and 3 d). The dry process is mainly controlled by the dry way and dry time. The air-dried and oven-dried are adopted widely. Although there is no universal standard for dry time t, the most common dry time are 12 h, 24 h, and 48 h. In addition, for the oven-dried type, the temperature is generally controlled below 105°C to reduce the temperature effect on mechanical properties of rocks [7, 8].

Based on the accelerated wet-dry method, many researchers have conducted the study on mechanical and physical properties of rock materials after cyclic wet-dry treatment [5, 7, 9, 10, 12–16], such as density, porosity, water absorption, slake durability index, P-wave velocity, static

uniaxial compression strength (UCS), tensile strength, and fracture toughness. Although it is impractical to test each property index of weathered rocks, it is universally accepted that cyclic wet-dry reduces both mechanical and physical properties of rock materials to varying degrees. As for physical properties, a substantial experiment concluded that, with the increasing wet-dry cycles, the P-wave velocity, density, and slake durability index show an increasing trend, while the porosity and water absorption increase due to the wet-dry induced by deterioration. In terms of mechanical properties, investigations were mainly concentrated on UCS, tensile strength, and fracture toughness. For example, the unconfined compression strength of sandstone specimens was measured by Hale and Shakoor [13] after 50 wet-dry cycles in total. They pointed out that there is no obvious reduction in UCS. Özbek [15], Khanlari and Abdilor [16], and Zhao et al. [17] obtained similar results after different wet-dry cycles. However, a sharp decrease in uniaxial compression strength (reduced by 86.1%, after 8 cycles), tensile strength (reduced by 73.42%, after 10 cycles), and fracture toughness (reduced by 52.4%, after 7 cycles) was reported by Yao et al. [18], Liu et al. [19], and Hua et al. [20], respectively. The main causes for this discrepancy are the different mineralogical composition and microstructure (e.g., voids, cementations, texture, and fissures), which affect the sensitivity to cyclic wet-dry treatment [17]. As the testing technique progresses, the wet-dry induced mechanism in the microscale has been visualized with the aid of micro-computed tomography (CT), scanning electron microscopy (SEM), and nuclear magnetic resonance (NMR). Zhang et al. [21], Zhou et al. [22], and Liu et al. [23] utilized the SEM technique to observe the microstructure of the rock specimen subjected to different wet-dry cycles and concluded that the combination of rock grains was weakened by the microcracks and argillization. Liu et al. [19] conducted a series of CT whole-section scanning on sandstone specimens under dry-wet cycles and obtained that with the increasing dry-wet cycles, the density decreases whereas the porosity increases. Water distribution in saturation and dry processes was concluded from NMR images by Zhou et al. [24]. The test results explained the tensile strength differences under the same water content but different water treatments.

However, the above research studies mainly focus on static mechanical and physical properties of rock materials. There is rare research on dynamic behaviors of weathered rock, especially the study on cyclic wet-dry cycles. Actually, rock materials may be broken dynamically to some extent in the engineering application, due to the impact loads induced by blasting, drilling, vibration, rock-bursts, or earthquake. Therefore, it is meaningful to study the dynamic properties of rocks subjected to cyclic wet-dry. Recently, researchers have paid attention to this issue. Zhou et al. [5, 22] analyzed the dynamic compression strength and dynamic tensile strength of sandstone after every 10 wet-dry cycles (50 cycles in total) by the modified split-Hopkinson pressure bar system and concluded that both dynamic compression and tensile strength decrease with the increase of wet-dry cycles. Considering combined effects of deterioration and loading rate in wet-dry cycles, a new decay model was established by Zhou et al. [22] to forecast the long-term dynamic tensile strength against many more cyclic wet-dry cycles. However, on account of varying rock types and different mechanical properties, more work should be done with cyclic wet-dry treatment and dynamic properties.

To investigate the cyclic wet-dry effect on static and dynamic compression properties of rocks, a series of experiments on red-sandstone were conducted after 0, 5, 10, 15, and 20 wet-dry cycles in this work. The dynamic compression tests were conducted by using the split-Hopkinson pressure bar system, of which the impact velocity was also considered to assess the loading rate effect in this study. The density, P-wave velocity, and the surface microscopic features were also analyzed to characterize the deterioration caused by cyclic wet-dry. Moreover, in order to reflect the loading rate and wet-dry cycles, a deterioration model was built to forecast the long-term dynamic compression strength of red-sandstone.

2. Materials and Methods

2.1. Specimen Preparations. In this study, red-sandstone specimens were selected from Linyi, Shandong province. Results of X-ray diffraction indicated that this kind of red-sandstone mainly consists of quartz (66.4%), feldspar (18.3%), calcite (8.6%), hematite (6.3%), and small amounts of chlorite, illite, and mica. Specimens were all extracted from the same red-sandstone block which has the good petrographic uniformity and geometrical integrity. Besides, ultrasonic detection was applied to minimize variations and guarantee good homogeneousness among specimens. According to the recommendation of International Society for Rock Mechanics (ISRM) [25, 26], red-sandstone was cut into normal cylinder specimens, $\Phi 50 \times 25$ mm for dynamic compression tests and $\Phi 50 \times 100$ mm for static compression tests, respectively. All the specimens were carefully polished to satisfy the dimensional standard suggested by the ISRM. Table 1 shows the essential strength and physical properties of red-sandstone.

2.2. Cyclic Wet-Dry Setup. In this study, a single wet-dry cycle was performed by submerging red-sandstone specimens into purified water for 24 hours. Then, specimens were dried in an oven for 24 hours with a constant temperature of 60°C and cooled to the room temperature. These specimens were divided into five groups, subjected to 0, 5, 10, 15, and 20 wet-dry cycles, for static and dynamic compression tests.

2.3. Ultrasonic and SEM Tests. As another physical property of rocks, the ultrasonic P-wave velocity is sensitive to inner microdeterioration caused by cyclic wet-dry. The P-wave velocity was measured by using a portable ultrasonic detector (RSM-SY6). It is developed by the Institute of Rock and Soil Mechanics, Chinese Academy of Science, with a primary frequency of 50 kHz and the sampling precision of 0.2 μs. Vaseline was applied to the top and bottom surfaces of specimens for a good coupling effect between the transmitter

Table 1: Variation of physical and strength properties of red-sandstone.

Density ($kg \cdot m^{-3}$)	Porosity (%)	P-wave velocity ($m \cdot s^{-1}$)	Compression strength (MPa)	Tensile strength (MPa)	Poisson's ratio
2478	0.45	2598	74.2	4.82	0.24

and the receiver. Besides, information of longitudinal waves was automatically recorded for the following analysis.

2.4. Mechanical Experiments. Static compression tests were conducted by using the rock mechanics testing system of RMT-150B. The loading mode was controlled by the displacement, and the loading rate was set at 0.05 mm/min. Displacements and loads were recorded automatically and processed for calculating the uniaxial compression strength.

As shown in Figure 1, the dynamic compression tests are performed by the SHPB test system of Φ50 mm. The SHPB system mainly consists of an incident bar, a striker bar, and a transmitted bar, with a length of 290 mm, 2400 mm, and 1400 mm, respectively. The specimen is placed between the incident and transmitted bars, which are composed of high strength 40Cr steel with an elastic modulus of 210 GPa and a density of 7800 kg/m^3. When the strike bar is launched with the help of a nitrogen gasholder, a compression longitudinal incident wave (ε_i) is formed at free end of the incident bar and propagated along with the incident bar soon afterwards. When reaching the bar-specimen interface, some of the waves propagate through the specimen and transmit to the transmitted bar (ε_t), whilst other waves are reflected back to the incident bar (ε_r). All waves are recorded by two strain gauges which are fixed on the incident bars and transmitted bars.

The shaping technique was employed to guarantee the dynamic equilibrium according to methods suggested by the ISRM [26, 27]. A soft rubber sheet was set on the free end of the incident bar as a pulse-shaping device, which was 1.0 mm in thickness and 10 mm in diameter. Figure 2 illustrates the typical impact pulse wave in the SHPB compression test. It can be clearly seen that the sum of incident wave and reflected wave is nearly equal to the transmitted wave, indicating that the stress equilibrium has been achieved during the impact process, and the inertial effect can be ignored [28, 29]. According to the 1D wave theory and verification of dynamic stress equilibrium, the dynamic parameters, such as stress, strain, and strain rate, can be calculated through the three-wave analysis [28].

3. Analyses and Results

3.1. Index Property Variations. The variation of P-wave velocity, density, and static uniaxial compression strength is listed in Table 2. The data clearly illustrate that, with the increase of wet-dry cycles, three index properties all decrease to varying degrees. After 20 wet-dry cycles, compared with untreated specimens, the density, P-wave velocity, and static UCS are reduced by 3.62%, 24.93%, and 18.28%, respectively. Besides, the most obvious decrease occurs in the P-wave velocity. Similar to many other studies [5, 22], it is found that the variation of three index properties changes quickly in the first few cycles, and then gets slowly with the increasing wet-dry cycles. It can be inferred that the first few wet-dry cycles have a greater responsibility for the rock deterioration.

Figure 3 shows typical static stress-strain curves of red-sandstone specimens subjected to different wet-dry cycles. It can be seen that curves under varying cycles are similar in shape, indicating an increasing trend with the increase of strain. When the strength reaches the maximum, there is a sharp drop, corresponding to the typical feature of brittle failure. Otherwise, in the initial stages, there is a compaction process, which is expressed with a concave curve. With the increasing wet-dry cycles, the compaction process is more obvious, resulting from the deterioration induced by wet-dry. The increasing critical strain also reflects this point. Above all, the rocks are more soft and ductile after the wet-dry treatments. This is primarily caused by the expansion and growth of internal microcracks.

3.2. Microscopic Observations. As discussed in Section 3.1, the cyclic wet-dry treatment has an adverse effect on the physical and mechanical properties of red-sandstone. To illustrate the deterioration mechanism induced by wet-dry cycles, the scanning electron microscope (SEM) technique was adopted to visualize the microstructure changes. Five cylinder samples with the dimension of 10 mm were prepared for the SEM test, before which samples were subjected to 0, 5, 10, 15, and 20 wet-dry cycles, respectively. Figure 4 shows typical SEM images of red-sandstone samples after different wet-dry cycles. It can be found that the microstructure of untreated specimen is intact, and loose granules [30–32] and new microcracks are hard to be observed (Figure 4(a)). For specimens subjected to 5 wet-dry cycles, a part of loose granules begin to separate from main grains, as shown in Figure 4(b). When 10 wet-dry cycles are reached, two new-formed microcracks are clearly seen around the grain (Figure 4(c)), demonstrating the partial failure of connection between two grains. With the increasing wet-dry cycles, not only the growth and expansion of microcracks but also the number and density of loose granules increase significantly, as shown in Figures 4(d) and 4(e). Additionally, microholes which are possibly caused by the dissolution of soft grains appear after 5 wet-dry cycles, as shown in Figures 4(c)–4(e). Due to the increasing microcracks and microholes, the grains, cements, or the connection between them are weakened or even destroyed, mainly resulting in the decay of physical and mechanical properties. The observation results are consistent with previous studies [5, 22, 23].

3.3. Dynamical Compression Strength of Red-Sandstone after Different Wet-Dry Cycles. After a range of tests

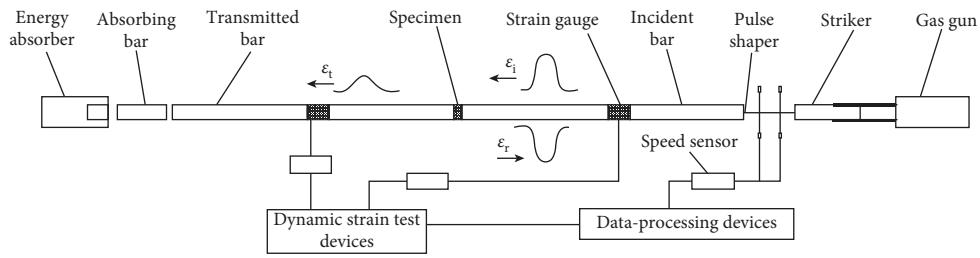

Figure 1: Schematics of SHPB system.

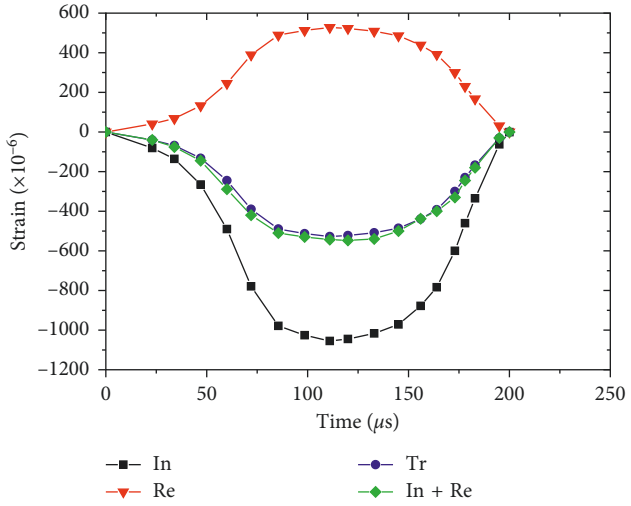

Figure 2: Dynamic stress equilibrium check in a typical dynamic compression test.

Table 2: Index properties variation of red-sandstone subjected to different wet-dry cycles.

W-D cycles	Dried density		P-wave velocity		Static UCS	
	After (g/cm^3)	Variation (%)	After (m/s)	Variation (%)	After (MPa)	Variation (%)
0	2478.0	0.00	2598.2	0.00	74.4	0.0
5	2438.2	−1.61	2350.0	−9.55	69.3	−6.85
10	2408.6	−2.80	2180.4	−16.08	67.1	−9.81
15	2396.7	−3.28	2020.3	−22.24	64.7	−13.04
20	2388.4	−3.62	1950.5	−24.93	60.8	−18.28

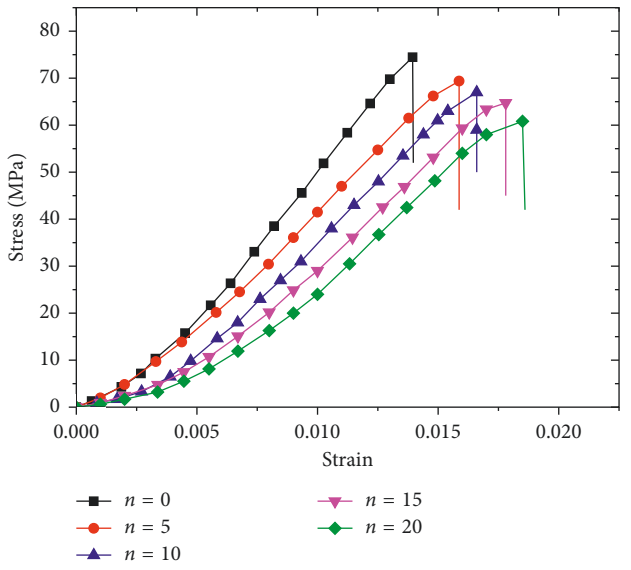

Figure 3: Strain-stress curves of red-sandstone with different wet-dry cycles.

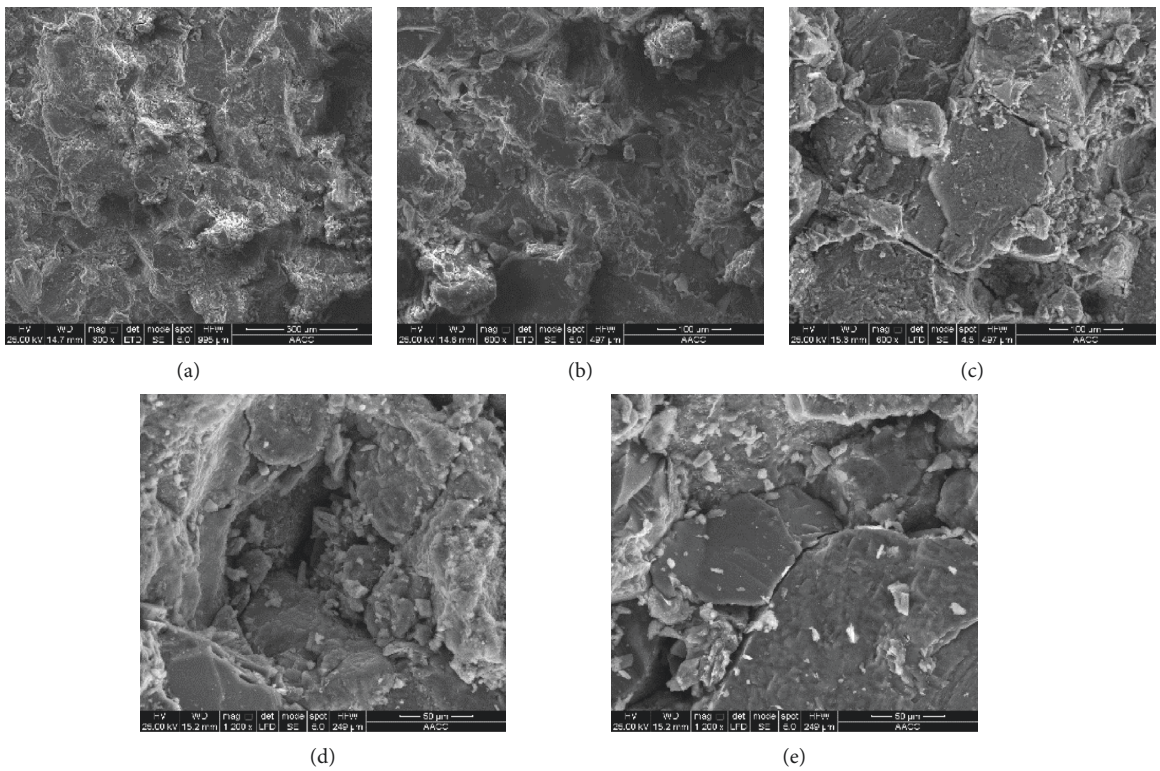

(a) (b) (c) (d) (e)

Figure 4: SEM images of red-sandstone free from and after different numbers of wet-dry cycles: (a) untreated specimen; (b) specimen after 5 wet-dry cycles; (c) specimen after 10 wet-dry cycles; (d) specimen after 15 wet-dry cycles; (e) specimen after 20 wet-dry cycles. Note that the magnification ratio is 1200.

and equilibrium verification on red-sandstone specimens subjected to different wet-dry cycles, the dynamic compression parameters are obtained, including the loading rate and dynamic compression strength, as shown in Table 3. Figure 5 deeply presents the variation of dynamic compression strength with the loading rate subjected to 0, 5, 10, 15, and 20 wet-dry cycles, respectively. The static compression strength is also included for a better comparison. As can be seen from Figure 5, the dynamic compression strength is affected not only by the loading rate but also by the number of wet-dry cycles. For specimens subjected to same wet-dry cycles, assuming that the dynamic compression strength of red-sandstone has an increasing trend with the increase of the loading rate, a significant loading rate-independent effect was observed. It was also observed that the increasing rate of dynamic strength increased quickly in the first few cycles, then increased slowly in the following cycles. Test results are in accordance with the previous literature by Zhou et al. [5]. For specimens under the similar loading rate, with the increase of wet-dry cycles, the dynamic compression strength decreases gradually. However, from the above data alone, it is impossible to conduct the quantitative research on strength reduction induced by wet-dry cycles, because loading rates are not the same under equal conditions. In order to solve this problem, exponential equations are adopted to fit variation rules of loading rate and dynamic compression strength. Figure 5 illustrates fitting curves, and the equations are listed as follows:

$$\begin{aligned}
&\sigma_d = 554.71 - 479.56e^{-0.00178\dot{\varepsilon}},\\
&R^2 = 0.99821, \qquad (n = 0),\\
&\sigma_d = 517.45 - 449.21e^{-0.00189\dot{\varepsilon}},\\
&R^2 = 0.99857, \qquad (n = 5),\\
&\sigma_d = 526.53 - 460.57e^{-0.00174\dot{\varepsilon}},\\
&R^2 = 0.99835\ , \qquad (n = 10),\\
&\sigma_d = 547.17 - 482.47e^{-0.00158\dot{\varepsilon}},\\
&R^2 = 0.99657, \qquad (n = 15),\\
&\sigma_d = 567.43 - 507.22e^{-0.00144\dot{\varepsilon}},\\
&R^2 = 0.99791, \qquad (n = 20),
\end{aligned} \tag{1}$$

where σ_d is the dynamic compression strength; $\dot{\varepsilon}$ and n are the loading rate and number of wet-dry cycles, respectively.

From the fitting results above, a good correlation coefficient is found between fitting curves and scatter points, indicating that the exponential equation can effectively reflect the nonlinear relationship between the loading rate and dynamic compression strength of red-sandstone exposed to different wet-dry cycles. To analyze wet-dry effects on dynamic properties, dynamic compression strength of specimens under the same loading rate ($100\,s^{-1}$, $150\,s^{-1}$, $200\,s^{-1}$,

Table 3: Dynamic compressive strength of red-sandstone with corresponding loading rate.

Specimen no.	n	Loading rate (s^{-1})	Strength (MPa)
DC0-1	0	106	157.7
DC0-2		118	164.3
DC0-3		138	180.2
DC0-4		153	193.7
DC0-5		168	195.7
DC0-6		182	208.5
DC0-7		206	223.0
DC0-8		215	229.4
DC0-9		229	234.3
DC0-10		248	248.9
DC0-11		269	256.2
DC0-12		286	269.1
DC0-13		296	270.2
DC1-1	5	103	146.3
DC1-2		121	158.7
DC1-3		138	170.4
DC1-4		154	182.3
DC1-5		175	196.8
DC1-6		183	198.8
DC1-7		213	215.4
DC1-8		238	234.5
DC1-9		243	235.6
DC1-10		262	246.6
DC1-11		275	250.4
DC1-12		289	256.8
DC1-13		308	266.9
DC1-14		314	266.0
DC2-1	10	97	136.3
DC2-2		116	149.0
DC2-3		135	159.4
DC2-4		149	168.5
DC2-5		168	183.7
DC2-6		175	188.4
DC2-7		193	199.6
DC2-8		235	220.2
DC2-9		249	228.9
DC2-10		258	236.0
DC2-11		274	238.0
DC2-12		293	248.6
DC2-13		315	257.3
DC2-14		326	265.8
DC3-1	15	105	136.8
DC3-2		116	143.6
DC3-3		132	163.7
DC3-4		145	162.4
DC3-5		159	168.5
DC3-6		174	179.7
DC3-7		213	199.0
DC3-8		226	209.3
DC3-9		237	216.9
DC3-10		252	224.2
DC3-11		269	232.4
DC3-12		272	234.0
DC3-13		303	249.6
DC3-14		319	251.6
DC3-15		336	264.3
DC4-1	20	113	136.5
DC4-2		128	145.0
DC4-3		142	152.1
DC4-4		158	163.2
DC4-5		174	170.0
DC4-6		182	178.9
DC4-7		209	190.6
DC4-8		223	200.3
DC4-9		231	206.4
DC4-10		246	214.2
DC4-11		263	217.2
DC4-12		278	230.5
DC4-13		296	236.6
DC4-14		317	243.0

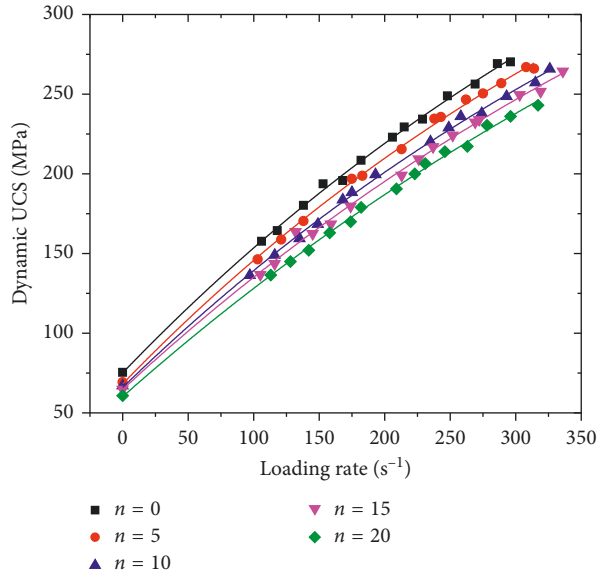

Figure 5: Dynamic compression strength against loading rate caused by different wet-dry cycles.

250 s^{-1}, and 300 s^{-1}) is obtained based on equation (1). Figure 6 further illustrates the relationship between dynamic compression strength and number of wet-dry cycles at different loading rates. It can be seen that, regardless of the loading rate, the dynamic compression strength decreases with the increasing wet-dry cycles, verifying the deterioration effect on dynamic compression strength of red-sandstone. In general, cyclic wet-dry treatment has an adverse effect on both static and dynamic compression strengths of red-sandstone.

3.4. Decay Function Model of Dynamic Compression Strength after Different Wet-Dry Cycles. Limited to many nonartificial factors, such as laboratory conditions, research grants, and test period, laboratory tests cannot simulate site conditions

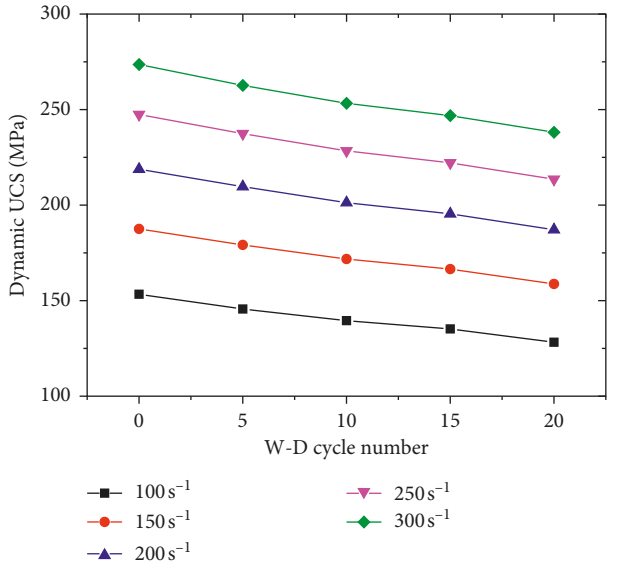

Figure 6: Dynamic compression strength against number of wet-dry cycles at different loading rates.

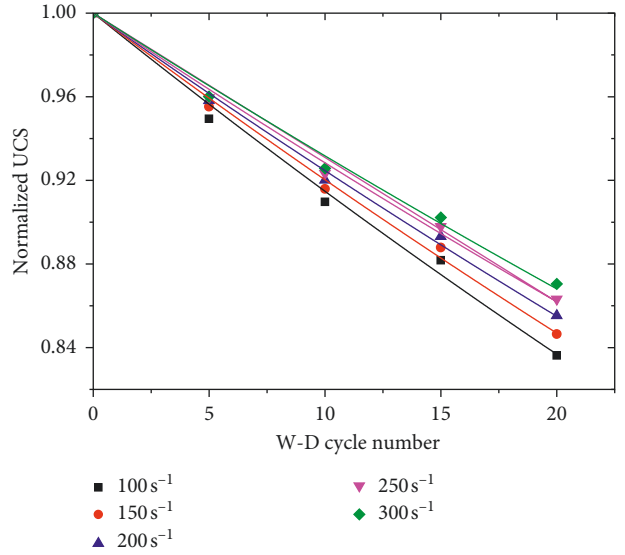

Figure 7: Normalized UCS against number of wet-dry cycles at different loading rates.

completely, especially the weathering time which can last for several years. Therefore, the long-term prediction which cannot be tested in laboratory condition for dynamic properties of rock is addressed. To conduct the long-term prediction for mechanical properties and provide a more reliable guidance for the design and construction in rock engineering, several decay models subjected to different weathering conditions were established [33–36]. For instance, to investigate the decay effect of rock against cyclic heating-cooling and freezing-thawing, a decay function model, consisting of decay constant (λ) and number of cycles (N), was proposed by Mutlutürk et al. [33], and the model was confirmed to satisfy the experimental data well. On the basis of this decay model, considering the strain rate, an improved deterioration model was proposed by Wang et al. [37, 38] for the prediction of dynamic mechanical degradation of rocks exposed to long-term weathering. According to loading rate and number of wet-dry cycles, the decay function model of red-sandstone against wet-dry cycles is presented as follows:

$$\sigma_{dn} = \sigma_{d0} e^{-\lambda(\dot{\varepsilon})n}, \tag{2}$$

where σ_{dn} is the dynamic compression strength against n wet-dry cycles; σ_{d0} is the initial dynamic compression strength free from wet-dry treatment; and $\lambda(\dot{\varepsilon})$ is the decay constant in consideration of the loading rate.

For a more straightforward understanding on the deterioration induced by wet-dry, the half-life ($n_{1/2}$), revealing that the number of wet-dry is needed to reduce the dynamic compression strength to its half, is also adopted in this paper, as follows:

$$n_{1/2} = \frac{\ln 2}{\lambda(\dot{\varepsilon})}. \tag{3}$$

Based on the above test data, the relationship between wet-dry cycles and normalized value of dynamic compression strength (i.e., σ_{dn}/σ_{d0}) is illustrated in Figure 7. With the aid of the regression analysis method, the value of σ_{dn}/σ_{d0} is the exponential fitted, and the decay constant (λ) and half-life value ($n_{1/2}$) are obtained, as listed in Table 4. As the decay constant and half-life value are associated with the loading rate, the relationship between two parameters and loading rate is illustrated in Figures 8 and 9, and the scatters are also exponential fitted, as expressed in equations (4) and (5). As can be seen from Figures 8 and 9, with the increase of the loading rate, λ decreases gradually whereas $n_{1/2}$ increases accordingly:

$$\begin{aligned} \lambda(\dot{\varepsilon}) &= 0.00533 + 0.00511e^{-0.00358\dot{\varepsilon}}, \\ R^2 &= 0.997, \end{aligned} \tag{4}$$

$$\begin{aligned} N_{1/2} &= 172.76 - 106.96e^{-0.0011\dot{\varepsilon}}, \\ R^2 &= 0.998. \end{aligned} \tag{5}$$

As illustrated above, the decay function model of red-sandstone against different wet-dry cycles with the loading rate is achieved by substituting equation (4) into equation (2):

$$\sigma_{dn} = \sigma_{d0} e^{-\left(0.00533+0.00511e^{-0.00358\dot{\varepsilon}}\right)n}. \tag{6}$$

4. Conclusions

In this paper, a series of static and dynamic compression tests after 0, 5, 10, 15, 20, and 25 wet-dry cycles were carried out, and the deterioration mechanism was explained through SEM. Besides, a decay function model taking the loading rate into account was developed for the long-term prediction of dynamic compression strength. The conclusions are as follows:

(1) Cyclic wet-dry treatment significantly affects the mechanical and physical properties of red-sandstone.

Table 4: Decay constant and half-life of dynamic UCS of red-sandstone after cyclic W-D cycles.

Loading rate (s^{-1})	100	150	200	250	300
Decay constant, λ ($\times 10^{-3}$)	8.91	8.31	7.83	7.43	7.07
Half-life, $N_{1/2}$	77.8	83.4	88.5	93.3	98.0

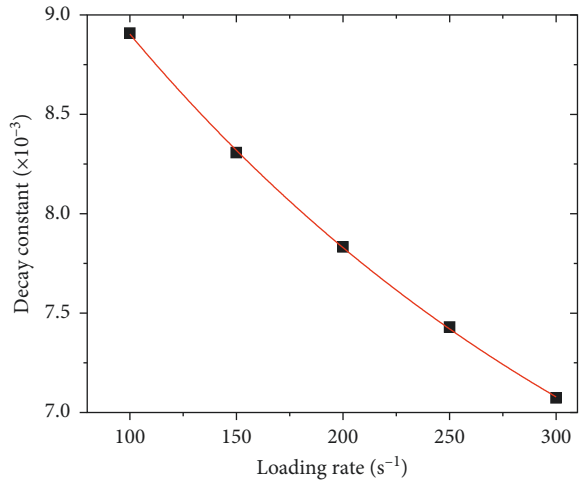

Figure 8: Variation of decay constant against loading rate.

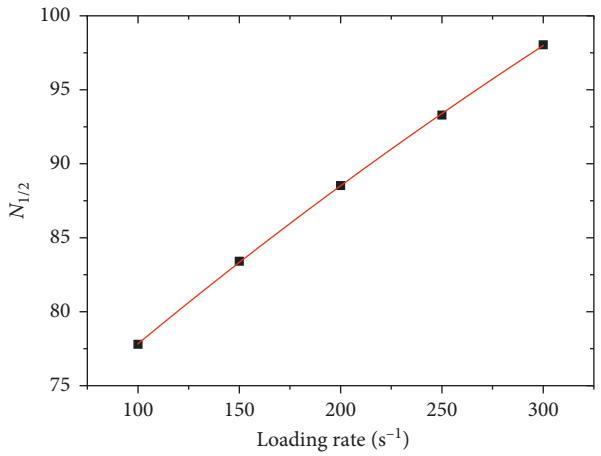

Figure 9: Variation of half-life value against loading rate.

With the increase of wet-dry cycles, the P-wave velocity, dried density, and static compression all decrease to varying degrees.

(2) Dynamic compression strength of red-sandstone is influenced by loading rate and number of wet-dry cycles. When the loading rate remains at a similar value, the dynamic compression strength decreases with the increase of wet-dry cycles. For specimens subjected to the same wet-dry cycles, the dynamic compression strength increases with the increasing loading rate.

(3) The SEM technique is adopted to study the microdeterioration mechanism due to cyclic wet-dry. The results indicate that the deterioration mainly contributes to the weaken connection between grains or cements, and the deterioration degree is also strengthened with the increase of wet-dry cycles.

(4) Considering the loading rate, a decay function model is proposed for the long-term prediction on dynamic compression strength of red-sandstone subjected to cyclic wet-dry. Two parameters, namely, the decay constant ($\lambda(\dot{\varepsilon})$) and half-life value ($n_{1/2}$), are expressed against the loading rate. It is concluded that the higher the loading rate, the smaller the value of λ, and the more cycles needed to reduce the strength to its half.

Data Availability

The data used to support the findings of this study are included within the article.

Conflicts of Interest

The authors declare that they have no conflicts of interest.

Acknowledgments

The work was supported by the National Natural Science Foundation of China (51323004 and 51704281), the Major Issues of Natural Science Research in Jiangsu Higher Education Institutions (17KJA560002), the Natural Science Foundation of Jiangsu Higher Education Institutions (17KJB440002 and 18KJB480003), and the Doctor Special Research Fund of Jiangsu Collaborative Innovation Center for Building Energy Saving and Construct Technology (SJXTBS1701 and SJXTBS1705). The corresponding author would like to thank the financial support by the State Key Laboratory for GeoMechanics and Deep Underground Engineering, China University of Mining & Technology (SKLGDUEK1805).

References

[1] M. J. Selby, *Hillslope Materials and Processes*, Oxford University Press, Oxford, UK, 1993.

[2] P. Reiche, *A Survey of Weathering Processes and Products*, University of New Mexico Publications in Geology, University of New Mexico Press, Albuquerque, NM, USA, 1950.

[3] A. Momeni, S. S. Hashemi, G. R. Khanlari, and M. Heidari, "The effect of weathering on durability and deformability properties of granitoid rocks," *Bulletin of Engineering Geology and the Environment*, vol. 76, no. 3, pp. 1037–1049, 2017.

[4] D. Ma, X. Cai, Z. Zhou, and X. Li, "Experimental investigation on hydraulic properties of granular sandstone and mudstone mixtures," *Geofluids*, vol. 2018, Article ID 9216578, 13 pages, 2018.

[5] Z. Zhou, X. Cai, L. Chen, W. Cao, Y. Zhao, and C. Xiong, "Influence of cyclic wetting and drying on physical and dynamic compressive properties of sandstone," *Engineering Geology*, vol. 220, pp. 1–12, 2017.

[6] K. Hall, "Rock moisture content in the field and the laboratory and its relationship to mechanical weathering studies," *Earth*

Surface Processes and Landforms, vol. 11, no. 2, pp. 131–142, 1986.

[7] K. Hall and A. Hall, "Weathering by wetting and drying: some experimental results," *Earth Surface Processes and Landforms*, vol. 21, no. 4, pp. 365–376, 1996.

[8] R. U. Cooke, "Laboratory simulation of salt weathering processes in arid environments," *Earth Surface Processes*, vol. 4, no. 4, pp. 347–359, 1979.

[9] G. Pardini, G. V. Guidi, R. Pini, D. Regüés, and F. Gallart, "Structure and porosity of smectitic mudrocks as affected by experimental wetting-drying cycles and freezing-thawing cycles," *CATENA*, vol. 27, no. 3-4, pp. 149–165, 1996.

[10] P. D. Sumner and M. J. Loubser, "Experimental sandstone weathering using different wetting and drying moisture amplitudes," *Earth Surface Processes and Landforms*, vol. 33, no. 6, pp. 985–990, 2008.

[11] M. L. Lin, F. S. Jeng, L. S. Tsai, and T. H. Huang, "Wetting weakening of tertiary sandstones-microscopic mechanism," *Environmental Geology*, vol. 48, no. 2, pp. 265–275, 2005.

[12] C. Gökceoğlu, R. Ulusay, and H. Sönmez, "Factors affecting the durability of selected weak and clay-bearing rocks from Turkey, with particular emphasis on the influence of the number of drying and wetting cycles," *Engineering Geology*, vol. 57, no. 3-4, pp. 215–237, 2000.

[13] P. A. Hale and A. Shakoor, "A laboratory investigation of the effects of cyclic heating and cooling, wetting and drying, and freezing and thawing on the compressive strength of selected sandstones," *Environmental and Engineering Geoscience*, vol. 9, no. 2, pp. 117–130, 2003.

[14] R. Doostmohammadi, M. Moosavi, T. Mutschler, and C. Osan, "Swelling pressure of mudstone under cyclic wetting and drying," in *Proceedings of 11th Congress of the International Society for Rock Mechanics*, Lisbon, Portugal, July 2007.

[15] A. Özbek, "Investigation of the effects of wetting-drying and freezing-thawing cycles on some physical and mechanical properties of selected ignimbrites," *Bulletin of Engineering Geology and the Environment*, vol. 73, no. 2, pp. 595–609, 2013.

[16] G. Khanlari and Y. Abdilor, "Influence of wet-dry, freeze-thaw, and heat-cool cycles on the physical and mechanical properties of Upper Red sandstones in central Iran," *Bulletin of Engineering Geology and the Environment*, vol. 74, no. 4, pp. 1287–1300, 2014.

[17] Z. Zhao, J. Yang, D. Zhang, and H. Peng, "Effects of wetting and cyclic wetting-drying on tensile strength of sandstone with a low clay mineral content," *Rock Mechanics and Rock Engineering*, vol. 50, no. 2, pp. 485–491, 2016.

[18] H. Y. Yao, Z. H. Zhang, and Z. H. Zhu, "Uniaxial mechanical properties of sandstone under cyclic of drying and wetting," *Advanced Materials Research*, vol. 243–249, pp. 2310–2313, 2011.

[19] X. Liu, Z. Wang, Y. Fu, W. Yuan, and L. Miao, "Macro/microtesting and damage and degradation of sandstones under dry-wet cycles," *Advances in Materials Science and Engineering*, vol. 2016, Article ID 7013032, 16 pages, 2016.

[20] W. Hua, S. Dong, Y. Li, J. Xu, and Q. Wang, "The influence of cyclic wetting and drying on the fracture toughness of sandstone," *International Journal of Rock Mechanics and Mining Sciences*, vol. 78, pp. 331–335, 2015.

[21] Z. Zhang, Q. Jiang, C. Zhou, and X. Liu, "Strength and failure characteristics of Jurassic Red-Bed sandstone under cyclic wetting-drying conditions," *Geophysical Journal International*, vol. 198, no. 2, pp. 1034–1044, 2014.

[22] Z. Zhou, X. Cai, D. Ma, L. Chen, S. Wang, and L. Tan, "Dynamic tensile properties of sandstone subjected to wetting and drying cycles," *Construction and Building Materials*, vol. 182, pp. 215–232, 2018.

[23] X. Liu, M. Jin, D. Li, and L. Zhang, "Strength deterioration of a Shaly sandstone under dry–wet cycles: a case study from the Three Gorges Reservoir in China," *Bulletin of Engineering Geology and the Environment*, vol. 77, no. 4, pp. 1607–1621, 2017.

[24] Z. Zhou, X. Cai, D. Ma et al., "Water saturation effects on dynamic fracture behavior of sandstone," *International Journal of Rock Mechanics and Mining Sciences*, vol. 114, pp. 46–61, 2019.

[25] D. Ma, X. Cai, Q. Li, and H.Y. Duan, "In-situ and numerical investigation of groundwater inrush hazard from grouted karst collapse pillar in longwall mining," *Water*, vol. 10, no. 9, p. 1187, 2018.

[26] Y. X. Zhou, K. Xia, X. B. Li et al., "Suggested methods for determining the dynamic strength parameters and mode-I fracture toughness of rock materials," *International Journal of Rock Mechanics and Mining Sciences*, vol. 49, no. 1, pp. 105–112, 2012.

[27] Z. Zhou, X. Li, A. Liu, and Y. Zou, "Stress uniformity of split Hopkinson pressure bar under half-sine wave loads," *International Journal of Rock Mechanics and Mining Sciences*, vol. 48, no. 4, pp. 697–701, 2011.

[28] F. Dai, S. Huang, K. Xia, and Z. Tan, "Some fundamental issues in dynamic compression and tension tests of rocks using split Hopkinson pressure bar," *Rock Mechanics and Rock Engineering*, vol. 43, no. 6, pp. 657–666, 2010.

[29] K. Xia and W. Yao, "Dynamic rock tests using split Hopkinson (Kolsky) bar system—a review," *Journal of Rock Mechanics and Geotechnical Engineering*, vol. 7, no. 1, pp. 27–59, 2015.

[30] D. Ma, M. Rezania, H. S. Yu, and H. B. Bai, "Variations of hydraulic properties of granular sandstones during water inrush: effect of small particle migration," *Engineering Geology*, vol. 217, pp. 61–70, 2017.

[31] D. Ma, J. Wu, Q. Li, H. B. Bai, and Z. Zhou, "Grain size distribution effect on the hydraulic properties of disintegrated coal mixtures," *Energies*, vol. 10, no. 5, p. 612, 2017.

[32] D. Ma, Q. Li, M. R. Hall, and Y. Wu, "Experimental investigation of stress rate and grain size on gas seepage characteristics of granular coal," *Energies*, vol. 10, no. 4, p. 527, 2017.

[33] M. Mutlutürk, R. Altindag, and G. Türk, "A decay function model for the integrity loss of rock when subjected to recurrent cycles of freezing-thawing and heating-cooling," *International Journal of Rock Mechanics and Mining Sciences*, vol. 41, no. 2, pp. 237–244, 2004.

[34] B. Fatih, "Predicting mechanical strength loss of natural stones after freeze-thaw in cold regions," *Cold Regions Science and Technology*, vol. 83-84, pp. 98–102, 2012.

[35] A. Jamshidi, M. R. Nikudel, and M. Khamehchiyan, "Predicting the long-term durability of building stones against freeze–thaw using a decay function model," *Cold Regions Science and Technology*, vol. 92, pp. 29–36, 2013.

[36] Q. S. Liu, S. B. Huang, Y. S. Kang, and X. W. Liu, "A prediction model for uniaxial compressive strength of deteriorated rocks due to freeze–thaw," *Cold Regions Science and Technology*, vol. 120, pp. 96–107, 2015.

[37] P. Wang, J. Y. Xu, S. Liu, S. H. Liu, and H. Y. Wang, "A prediction model for the dynamic mechanical degradation of sedimentary rock after a long-term freeze-thaw weathering: considering

the strain-rate effect," *Cold Regions Science and Technology*, vol. 131, pp. 16–23, 2016.

[38] P. Wang, J. Xu, X. Fang, M. Wen, G. Zheng, and P. Wang, "Dynamic splitting tensile behaviors of red-sandstone subjected to repeated thermal shocks: deterioration and micromechanism," *Engineering Geology*, vol. 223, pp. 1–10, 2017.